Photoblinking of Rhodamine 6G in Poly(vinyl alcohol): Radical Dark State Formed through the Triplet

Rob Zondervan, Florian Kulzer, Sergei B. Orlinskii, and Michel Orrit*

Molecular Nano-Optics and Spins (MoNOS), Leiden Institute of Physics (LION), Huygens Laboratory, Leiden University, P.O. Box 9504, 2300 RA Leiden, The Netherlands

Received: March 20, 2003; In Final Form: June 16, 2003

We investigate the fluorescence intensity of rhodamine 6G in poly(vinyl alcohol) as a function of excitation intensity, illumination time, the presence of oxygen, and temperature. The variations in emissivity (or fluorescence brightness) are attributed to a dark state, which shows populating kinetics resembling those of the triplet state, but a much longer lifetime. We simulate the observed kinetics by a four-level model, in which a long-lived dark state is formed through the triplet as an intermediate state. The weak temperature dependence of the lifetime of the dark state points to electron tunneling as the main recovery process. This intermolecular mechanism also explains the observed broad distribution of lifetimes. An electron-spin-resonance experiment confirms the assignment of the dark state to a radical. For the first time, photoinduced charge transfer is identified as a source of blinking in single-molecule measurements.

Introduction

Single fluorescing quantum systems almost invariably display blinking, i.e., discrete fluctuations of their fluorescence intensity with time.[1] Blinking is generally interpreted as arising from transitions of the fluorophore to a nonfluorescing or less-fluorescing state, a "dark" or "dim" state, from which it returns to the initial state after some time.[2] If the system does not return to the fluorescing state, the process is called bleaching. If blinking is induced by the excitation light, we call it photoblinking. Photoblinking can be observed in an ensemble experiment, albeit indirectly, because the transitions of all molecules can be synchronized by intensity variations of the excitation laser. High peak intensities and pulsed excitation are usually needed to induce significant photoblinking,[3−6] but here we use continuous excitation, shutters, and time-resolved detection. Blinking of single fluorophores can be investigated in two ways. From the fluorescence time trace of a single molecule (or single particle) on- and off-times can be determined by defining a threshold between the fluorescent "on"-level and the nonfluorescing or less-fluorescent "off"-level. The times the molecule is either "on" or "off" provide direct information on the population rate(s) of the involved dark state(s), the recovery rate(s), and the distributions of those rates.[7−10] An alternative method is to measure the fluorescence autocorrelation function, which yields equivalent information without the necessity to define an arbitrary threshold between on- and off-levels.[11−15]

For single organic dye molecules, photoblinking is commonly related to excursions of the molecules to the triplet state. Triplet photoblinking is characterized by a succession of relatively short on- and off-times, typically on the order of microseconds to a few milliseconds.[7,9,10,12,16−22] The off-times are sensitive to the presence of oxygen, which drastically shortens the triplet lifetime.[12,21] In solid matrixes, more complex blinking behavior has been observed with much longer off-times than expected from a triplet bottleneck (up to minutes).[7−13,22−31] Besides the triplet state, other metastable excited states and/or thermally induced changes of the electronic ground state[8,11] are commonly assumed to be involved. Proposed mechanisms are (i) Photochemical processes such as photoionization followed by electron trapping,[23,25,26,30] photoisomerization,[22] or reversible oxidation by oxygen.[30] (ii) Fluorescence quenching by other molecules.[9,23] (iii) Conformational changes of the molecule, which can be either photophysical[7,31] or thermally induced.[8,11] (iv) Rotation of the molecule.[13,22−24,31] (v) Spectral changes induced by the environment of the molecule, either by structure[9,23] and/or polarity[7] fluctuations of the host matrix, by spatial heterogeneities in the matrix structure,[8,28] or by desorption and reabsorption of the molecule when it is on a surface.[24] In some cases,[12,27,29] off-times of approximately 100 ms or longer have been interpreted as excursions to the triplet state. As the triplet lifetime of dyes usually does not exceed a few milliseconds in an inert atmosphere, this explanation would require an unlikely large spread or change of this lifetime by several orders of magnitude.

Here, we report on the reversible decrease (by up to a factor of 20) of the fluorescence brightness of large ensembles of rhodamine 6G molecules in poly(vinyl alcohol) under continuous-wave excitation. We investigate the influence of excitation intensity, temperature, and the presence of oxygen. We develop a model for photoblinking along with the description of our results and draw conclusions on the nature of the dark state involved and on the consequences of the long off-times for single-molecule microscopy.

Experimental Section

The system under investigation is the ionic dye rhodamine 6G (R6G, cf. Figure 1) in solid poly(vinyl alcohol) (PVA). A solution of R6G (Radiant Dyes laser grade with counterion BF_4^-) in methanol (HPLC-grade) is added to a 1 wt % solution of PVA ($M_W = 1.25 \times 10^5$ g/mol) in 1:1 methanol−water such that the concentration of R6G is 2.0×10^{-5} M with respect to the volume of the PVA. This solution is spin-coated on a fused-quartz plate, which is used because of its low fluorescence background. The sample is characterized by measuring the

* Corresponding author. E-mail: orrit@molphys.leidenuniv.nl.

10.1021/jp034723r CCC: $25.00
Published on Web 08/06/2003

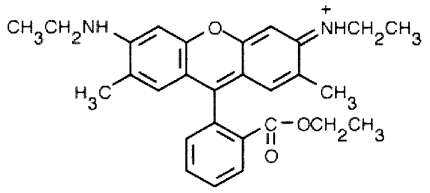

Figure 1. Structure of rhodamine 6G.

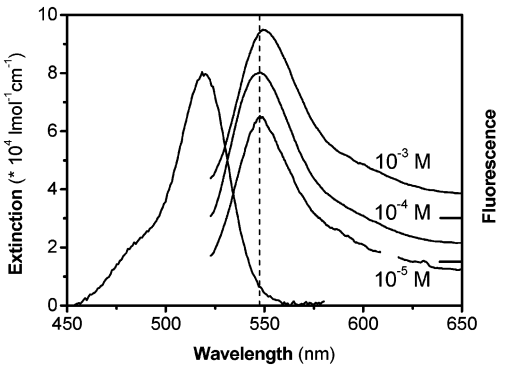

Figure 2. Absorption spectrum (on the left) and fluorescence spectra at various concentrations (on the right) of rhodamine 6G in poly(vinyl alcohol). A vertical offset between the fluorescence spectra is introduced for clarity. In the fluorescence spectrum at 10^{-5} M, a Raman line from the PVA matrix at 620 nm has been removed. The dashed line indicates the maximum of the fluorescence spectra at 10^{-4} and 10^{-5} M as a guide to the eye. The maximum at 10^{-3} M is slightly red-shifted.

absorption spectrum on a commercial absorption spectrometer (Perkin-Elmer Lambda 16) and fluorescence spectra at various concentrations with an Acton 500i spectrograph equipped with a back-illuminated CCD camera (Princeton Instruments Spec-10:400B) (cf. Figure 2). From the absorption spectrum, we obtain the absorption cross section of R6G in PVA, (3.0 ± 0.3) Å^2, at 514.5 nm.

The experiments on the fluorescence dynamics are performed in a flow cryostat (Leybold Heraeus) to control the atmosphere (air, nitrogen, or helium) and the temperature. Nitrogen and helium are obtained from evaporation of respectively liquid nitrogen and helium. The air is retrieved from a pressurized air supply with a constant relative humidity of approximately 15%. At room temperature, the experiments are performed under continuous flow. At low temperatures, the cryostat is filled with the desired atmosphere. The temperature is varied between 295 and 10 K.

The optical setup resembles a low-resolution confocal microscope. The system is excited with the 514.5 nm line of an argon-ion laser (Spectra-Physics Stabilite 2017), whose intensity is tuned by a Newport M925B variable attenuator. The excitation beam passes an optical shutter (Uniblitz, Vincent Associates), a beam expander (1:4), and a laser-line cleanup filter (Laser Components LCS10-515-F). The excitation beam is focused by an achromatic lens with a focal length of 80 mm, which also serves to collect the fluorescence. The excitation and fluorescence photons are separated by a dichroic beam splitter (AHF Analysentechnik HQ530LP) and in the detection path an additional notch-filter centered on 514.5 nm (Kaiser Optical Systems HNPF-514.5) suppresses residual excitation light. A spatial filter consisting of a lens with a focal length of 250 mm and a 150 μm pinhole further selects the fluorescence from the excitation spot. The fluorescence is monitored with a digital photomultiplier tube, EMI 9558AM 20143, the output pulses of which are discriminated (EG&G Parc model 1182) and fed into a TTL counter input of the control electronics (ADWin-Gold from Keithley Instruments). The excitation light transmitted through the sample holder is detected by a Hamamatsu S2386-45K photodiode for normalization.

For a quantitative analysis of fluorescence time traces, all molecules should experience (as far as possible) the same laser intensity. If the sample dimensions do not exceed the center of the beam by more than half the full width at half-maximum (fwhm) of the Gaussian spot, the intensity variation across the sample is less than 15%. To restrict the sample dimensions, we cover it with a pinhole-array mask of stainless steel (10×10 laser-drilled holes, manufactured in the Laser Centre of Loughborough College). The holes are separated by 240 μm and have a diameter of 40 μm. An excitation spot with a fwhm of approximately 80 μm on the sample is obtained by slightly defocusing the beam expander. The holes can be addressed individually by means of a manual scan mirror.

To directly compare time traces recorded at different excitation intensities, we normalize the measured fluorescence intensity by the excitation intensity. This normalized quantity is defined as the *emissivity* of the ensemble. Moreover, because the area of the holes and the thickness of the polymer film may fluctuate, we normalize this emissivity to the one measured at the same hole at 65 mW/cm^2, the lowest intensity for which fluorescence can be measured with satisfactory signal-to-noise ratio.

In this paper, we present the results of three types of optical experiments. First, the decay kinetics of the fluorescence of R6G in PVA are studied by monitoring the emissivity as a function of the illumination time. Excitation intensities between 65 mW/cm^2 and 320 W/cm^2 are applied, and the time resolution varies from 1 to 100 ms. Second, the steady-state fluorescence level is determined. In this experiment, the observation time is in general limited by photobleaching. Third, we study the recovery kinetics of the emissivity after illumination, by applying a high excitation intensity during a short interval, typically 100 ms, then "instantaneously" reducing it to a lower value by means of an acousto-optical modulator (Quantum Technology 305).

To check the proposed hypothesis of light-induced radical formation, we perform an electron-spin-resonance (ESR) experiment with a pulsed ESR spectrometer developed in our laboratory and operating at a microwave frequency of 95 GHz (W-band).[32] In a pulsed ESR experiment, resonances between the magnetic sublevels of an electron spin and the microwave field are detected via the intensity of an electron-spin-echo (ESE).[33]

Results and Discussion

Figure 2 shows the absorption spectrum of 10^{-4} M R6G in PVA and fluorescence spectra at three different concentrations, from 10^{-3} to 10^{-5} M. The fluorescence spectra resemble the mirror image of the absorption spectrum, which suggests that the fluorescence arises from isolated dye molecules. Nevertheless, upon a closer look, the spectrum at 10^{-3} M appears to be slightly red-shifted with respect to the other two, which we attribute to the onset of fluorescence resonant-energy transfer (FRET) between the R6G molecules. The characteristic distance for FRET is given by the Förster radius, which for two R6G molecules is approximately 5 nm.[34] Assuming the R6G molecules to be randomly distributed in the sample, we can calculate the percentage of R6G molecules within 5 nm from one another.[35] For a concentration of 10^{-3} M, 27% of the R6G molecules have a neighbor within the Förster radius. At 10^{-4} M, this fraction becomes 3%, and we expect FRET to become negligible. Indeed, comparing the two low-concentration spectra of Figure 2, we find no shift, as expected for samples consisting

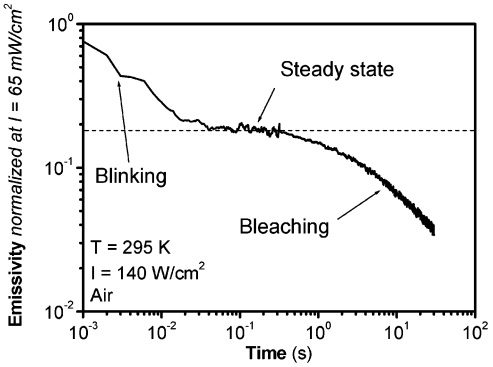

Figure 3. Typical emissivity time trace of rhodamine 6G in poly(vinyl alcohol) displaying three different stages in the millisecond to seconds time range. The first part shows a reversible decay of the emissivity related to photoblinking of the individual molecules. In the second part the emissivity reaches a plateau (dashed line), which reflects a steady state of the fluorescent population. The third part corresponds to an irreversible decay of the emissivity caused by photobleaching.

of isolated R6G molecules. Although this analysis does not exclude the presence of R6G dimers or aggregates, we may conclude that their contribution to the fluorescence can be ignored. A comparable study[36] of fluorescein (a dye similar to R6G) in PVA also showed that no significant intermolecular effects such as FRET occur at concentrations below 10^{-3} M.

Figure 3 shows a typical example of the time dependence of the emissivity of R6G in PVA in the millisecond to seconds time range after unblocking the laser. Three regimes can be distinguished in the trace. First the emissivity decreases within some tens of milliseconds, then it remains constant for approximately a second before it decreases further. The first decay is reversible. Switching off the excitation light for a few minutes after the emissivity has reached its plateau (second stage) leads to a complete recovery of its initial level. The reversible decay of the emissivity is related to photoinduced excursions of the molecules to a dark state; in other words, it reflects the photoblinking of the individual molecules. The plateau value of the second stage corresponds to the emissivity of the system in the (intensity dependent) steady state. The decay on the time scale of seconds is irreversible and is due to photobleaching. The separation of the time scales of photoblinking and photobleaching allows us to analyze the photoblinking without having to take bleaching into account. Even at the highest excitation intensity, 320 W/cm^2, the three stages in the decay of the emissivity are discernible.

Decay Kinetics of the Emissivity. To a good approximation, the fast reversible decay of the emissivity turns out to be single-exponential for each excitation intensity. Figure 4a displays an example of such a fit. We thus extract an effective decay rate k and evaluate this rate as a function of excitation intensity for various atmospheres and temperatures. Figure 4b shows the variation of k with intensity for air and nitrogen atmosphere at 295 K. Both curves are linear in the range of applied intensities and have the same slope. At lower temperatures, the same decay rates are observed. The single-exponential character of the decay indicates that the dispersion of the response times of the irradiated molecules is less than 1 order of magnitude. Besides the implications for the system itself, which we will discuss in the following paragraph, it shows that dispersion related to the excitation conditions can be neglected. We conclude that the presence of the pinhole-array mask (cf. Experimental Section) is sufficient to create a homogeneous excitation profile over the illuminated sample. Furthermore, the dispersion arising from the random orientations of the chromophores with respect to

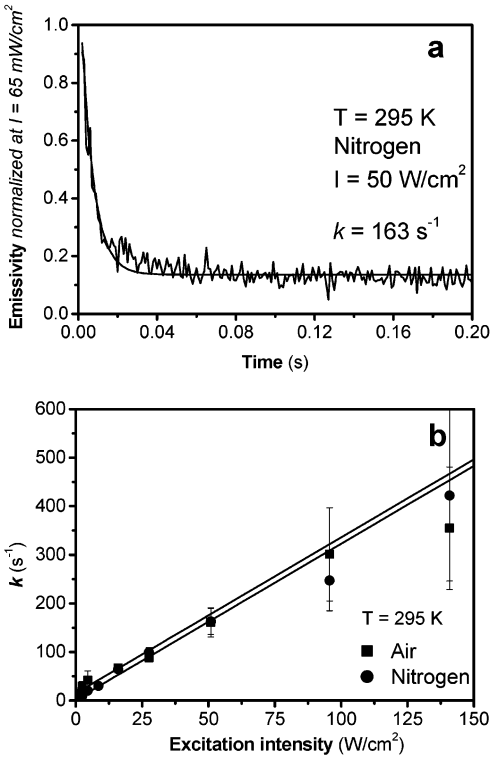

Figure 4. (a) Example of a single-exponential fit to a reversible emissivity decay. (b) Effective decay rate k of the emissivity as a function of the excitation intensity in air and nitrogen at 295 K.

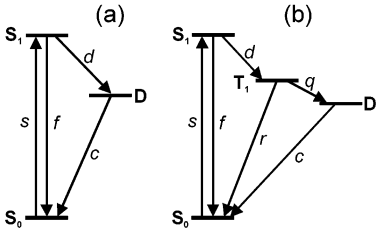

Figure 5. (a) Schematic energy-level diagram of a three-level system, consisting of the electronic ground state (S_0), the first excited singlet state (S_1) of rhodamine 6G and an a priori unspecified dark state (D). The symbols along the arrows refer to the rate constants of the respective transitions. (b) Same scheme for a four-level system consisting, besides the two singlet states (S_0 and S_1), of the lowest triplet state (T_1) of rhodamine 6G and of another dark state (D) populated through T_1.

the linearly polarized excitation light can be disregarded. A similar conclusion was reached earlier in hole-burning studies.[37,38]

To interpret the observed reversible decay, let us first assume the presence of a single dark state. We take three electronic energy levels of R6G into account, the singlet ground state (S_0), the first excited singlet state (S_1), and a dark state (D) of an a priori unspecified nature. Figure 5a presents the corresponding schematic energy-level diagram with the relevant transition rates, s, f, d, and c.

At intensities much below saturation of the optical two-level system, the pump rate s may be written

$$s = \sigma N I \tag{1}$$

where σ is the absorption cross section of R6G in PVA at 514.5 nm (3.0×10^{-16} cm^2), N is the number of photons in 1 J at 514.5 nm (2.59×10^{18} photons/J), and I is the excitation intensity (in W/cm^2). The fluorescence decay rate f equals 2.5×10^8 s^{-1}.[3]

From the kinetic equations for the respective populations, we obtain the emissivity Φ_{3LS} of the three-level system, which is proportional to N_{S_1}, the population of S_1:

$$\Phi_{3LS} = \frac{\eta}{I} N_{S_1} \tag{2}$$

with η the fluorescence quantum yield of R6G. In the three-level system there are two time scales, a fast one on the order of nanoseconds (related to the fluorescence decay rate *f)* and a slow one (related to the buildup of population in D, i.e., to *c* and *d*). With our time resolution we only observe the kinetics related to D, which means that the population of S_1 instantaneously adapts to changes in D. Consequently, we may use the so-called intermediate-state approximation and put the time-derivative of N_{S_1} to zero in the system of kinetic equations. Under the assumption that *f* is considerably larger than *d*, we obtain for the emissivity Φ_{3LS}:

$$\Phi_{3LS}(s,t) = A_{3LS} + B_{3LS} \exp(-k_{3LS} t) \tag{3a}$$

$$A_{3LS} = \frac{\sigma N \eta}{f} \frac{1}{1 + \frac{s}{f}\left(1 + \frac{d}{c}\right)} \tag{3b}$$

$$B_{3LS} = A_{3LS} P_{2LS} \frac{d}{c} \tag{3c}$$

$$k_{3LS} = P_{2LS} d + c \tag{3d}$$

$$P_{2LS} = \frac{s}{f + s} \tag{3e}$$

The rate k_{3LS} (3d) is the effective decay rate in this three-level model. As the reversible decay is found to be single-exponential, k_{3LS} is not dispersed and reflects a single value of the population rate *d* (because *c* is negligible in the applied intensity range, cf. Figure 4b). Applying the expression for k_{3LS} to fit the curves in Figure 4b, we obtain a value of approximately 1.0×10^6 s^{-1} for *d*. The fact that *d* is independent of atmosphere and temperature suggests that we are dealing with the intersystem crossing (ISC) rate from S_1 to the lowest triplet state (T_1). In principle, the ISC rate of R6G can be enhanced by the presence of oxygen depending on the S_1-T_1 gap, but this effect is negligible at the oxygen concentration of air.[39] The value of *d* is indeed in reasonable agreement with the ISC rates of R6G reported in the literature, which are in the range of 4.0×10^5 to 6.0×10^5 s^{-1}.[3,4] The discrepancy is most likely due to the inherent uncertainty in the determination of the absolute intensity, which is used to calculate *s* in eq 1.

For vanishing intensity, the decay rate k_{3LS} tends to *c*, the recovery rate from the dark state. If the dark state was T_1, cf. Figure 5a, the reported triplet lifetimes of about 400 μs (rate $= 2.5 \times 10^3$ s^{-1}) in an inert atmosphere[3] and of about 4 μs (rate $= 2.5 \times 10^5$ s^{-1}) in air (value for R6G in ethanol)[19] would lead to much higher rates than measured. Therefore, the low values of the decay rate (on the order of 10 s^{-1} at low intensity) indicate that the triplet state cannot be solely responsible for the observed photoblinking. Another dark state with longer lifetime has to be involved, as our discussion of the steady-state emissivity will also show.

Steady-State Emissivity. Figure 6 shows the steady-state emissivity, deduced from the plateau between the reversible decay and the photobleaching (cf. Figure 3), as a function of excitation intensity in air and nitrogen atmosphere at room temperature. The normalized steady-state emissivity drops by a factor of up to 5 in air and 10 in nitrogen at high intensity. The steady-state emissivity in helium atmosphere at 295 K displays the same intensity dependence as in nitrogen. Figure 7 presents the steady-state emissivity as a function of excitation intensity at various temperatures down to 10 K. At the lowest temperature the normalized steady-state emissivity decreases by a factor of up to 20 at high intensity. The effect of the temperature seems to be smaller than that of oxygen. The main emissivity changes occur between 295 and 80 K, as the data at 80 and 10 K are nearly indistinguishable.

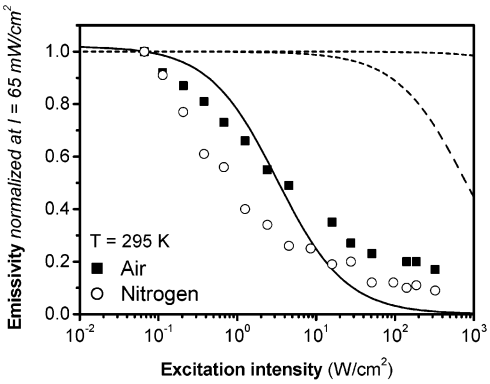

Figure 6. Steady-state emissivity of rhodamine 6G in poly(vinyl alcohol) as a function of excitation intensity in air and nitrogen atmosphere at room temperature. The dashed lines are simulations of the steady-state emissivity in the three-level model with the rates associated to the triplet state[3,19] in nitrogen (lower trace) and air (upper trace). The solid curve is a simulation for the three-level system with a lower recovery rate $c = 10$ s^{-1} of the dark state.

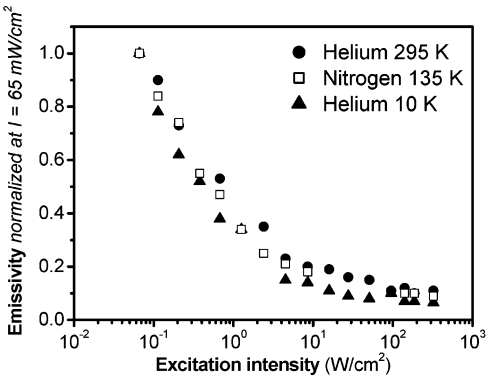

Figure 7. Steady-state emissivity as a function of excitation intensity at various temperatures in inert atmosphere. The plot at 10 K is indistinguishable within experimental error from that at 80 K.

For the three-level system the steady-state emissivity is equal to A_{3LS} (3b). The normalized steady-state emissivity Ψ_{3LS} is given by

$$\Psi_{3LS}(s) = \frac{A_{3LS}(s)}{A_{3LS}(s_0)} \tag{4}$$

where s_0 represents the pump rate at $I = 65$ mW/cm^2. Figure 6 shows simulations of the normalized steady-state emissivity Ψ_{3LS} with the published triplet lifetimes[3,19] in nitrogen and air at room temperature. These simulations strongly disagree with the experimental data, which confirms our earlier conclusion that the triplet is not the only dark state involved in the photoblinking.

To account for our data, we now consider a four-level system, in which T_1 is the intermediate state between S_1 and another dark state D, as illustrated in the energy level diagram of Figure 5b. In this model, D has the lower energy of the two dark states,

as its lifetime apparently determines the recovery, and T_1 is involved as the doorway state, because the effective population rate of D is found to be roughly equal to the ISC rate of R6G. In other words, ISC is the rate-limiting step in the formation of D, from which we conclude that q is larger than d. Realizing that r is on the order of d in air and even smaller in an inert atmosphere, there will be no buildup of steady-state population in T_1. As a result, the system (cf. Figure 5b) is expected to effectively reduce to a three-level system (Figure 5a), and the corresponding expressions (3) and (4) can be applied, with a new value of c.

The expression describing the time dependence of the emissivity Φ_{4LS} of the proposed four-level system is found from the corresponding rate equations by applying the intermediate-state approximation for the rate equations related to both S_1 and T_1. This is justified for T_1, because the lifetime of T_1 is much smaller than that of D. Neglecting d with respect to f, we obtain

$$\Phi_{4LS}(s,t) = A_{4LS} + B_{4LS}\exp(-k_{4LS}t) \tag{5a}$$

$$A_{4LS} = \frac{\sigma N \eta}{f}\frac{1}{1+\frac{s}{f}\left(1+\frac{d(q+c)}{c(q+r)}\right)} \tag{5b}$$

$$B_{4LS} = A_{4LS}P_{3LS}\left(\frac{dq}{c(q+r)}\right) \tag{5c}$$

$$k_{4LS} = P_{3LS}d + c \tag{5d}$$

$$P_{3LS} = \frac{s}{f+s\left(1+\frac{d}{q+r}\right)} \tag{5e}$$

For q much larger than r and d, (5b), (5c), and (5e) reduce to the corresponding equations for the three-level system, (3b), (3c), and (3e). The effective decay rate is indeed given by (3d), where c is now the recovery rate from the long-lived dark state D, and the normalized steady-state emissivity is again given by (4).

Figure 6 shows a simulation of the normalized steady-state emissivity with $c = 10\ s^{-1}$. The observed steady-state emissivity decays more slowly than the simulation. The discrepancy between data and model is significant. The experimental points are quite reproducible, as indicated by their limited scattering. We assign this deviation to a distribution of c values. Because the deviation extends over 3 decades of intensity at least, the distribution has to be broad. Several analytical expressions for the rate distribution may fit our data within the experimental accuracy. We obtain a satisfactory agreement with a power-law distribution of c between c_1 and infinity, which involves only two parameters, the exponent α and the cutoff c_1:

$$p(c) = \frac{\alpha}{c_1}\left(\frac{c_1}{c}\right)^{1+\alpha} \qquad \left(\int_{c_1}^{\infty} p(c)dc = 1\right) \tag{6}$$

After introducing this distribution, the normalized steady-state emissivity becomes

$$\Psi_{4LS}'(s) = \frac{\int_{c_1}^{\infty} p(c)\, A_{3LS}(s)\, dc}{\int_{c_1}^{\infty} p(c)\, A_{3LS}(s_0)\, dc} \tag{7}$$

with two fit parameters, c_1 and α.

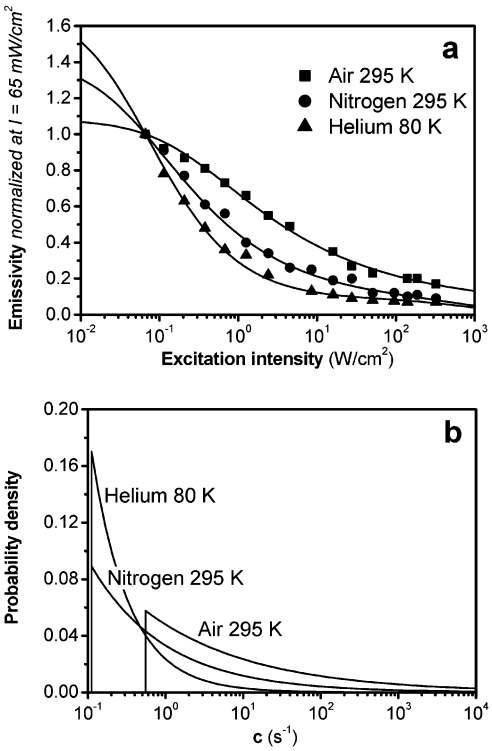

Figure 8. (a) Fits of three representative curves of the steady-state emissivity as a function of the excitation intensity. In these fits, the parameter c is described by power-law distributions as indicated in Figure 8b. For all three fits, we suppose that 5% of the population has only T_1 as the dark state. (b) Graphic representations of the applied power-law distributions of c to fit the steady-state curves shown in Figure 8a. The values of the fit parameters are in air at room-temperature, $c_1 = 0.5\ s^{-1}$ and $\alpha = 0.31$, in nitrogen at room-temperature, $c_1 = 0.1\ s^{-1}$ and $\alpha = 0.45$, and in helium at 80 K, $c_1 = 0.1\ s^{-1}$ and $\alpha = 0.90$.

To fit the steady-state curves, we have to assume that 5% of the molecules do not go into D at all ($q = 0$). The fits of three typical steady-state curves are presented in Figure 8a, for air and nitrogen at 295 K and for helium at 80 K. Figure 8b shows the distributions of c applied in these fits. The lifetime of D ($1/c$) is shorter in air than in inert atmosphere, and it lengthens when the temperature decreases. The narrowing of the distributions for inert atmosphere and low temperature (cf. Figure 8b) with respect to that for air is probably related to experimental constraints on the value of the cutoff rate c_1. For the first two, the respective distributions may partially consist of rates smaller than $0.1\ s^{-1}$, the smallest deducible recovery rate under our experimental conditions, whereas for air our experimental window allows us to observe the full range of rates.

Recovery of the Emissivity. As an independent test of our model, we verify that it correctly accounts for the recovery kinetics of the emissivity. We measure these kinetics by applying an AOM to switch "instantaneously" between high and low intensities. Figure 9 shows the results in air and nitrogen at room temperature and in helium at 80 K. The signal-to-noise ratio is rather poor because the light intensity is chosen as low as possible to get as close as possible to the ideal recovery, in the dark. With the parameters obtained from the steady-state curves (cf. Figures 8a and 8b), the recovery traces are simulated satisfactorily, as the solid lines in Figure 9 show.

Nature of the Dark State. First, we argue that the ambient relative humidity does not affect our experiments. In a recent paper, Hou and Higgins[31] point out that humidity may affect the blinking of a dye incorporated in a hydrophilic matrix like

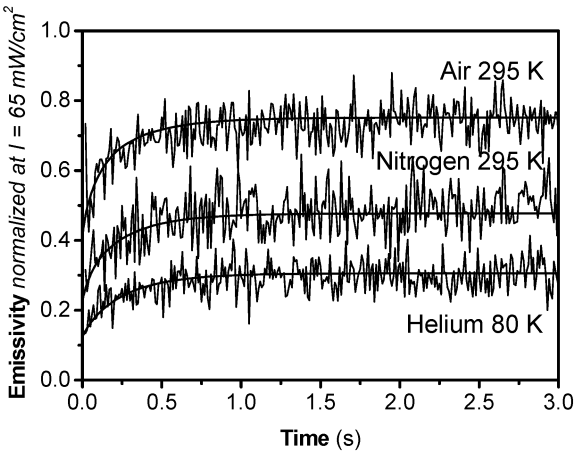

Figure 9. Recovery traces recorded in air at room temperature by switching from 8.0 to 0.6 W/cm^2 (upper trace), in nitrogen at room temperature by switching from 8.0 to 0.8 W/cm^2 (middle trace), and in helium at 80 K by switching from 8.0 to 0.9 W/cm^2 (lower trace). The solid lines are simulations with the parameters obtained from the fits of the steady-state curves (cf. Figures 8a and 8b).

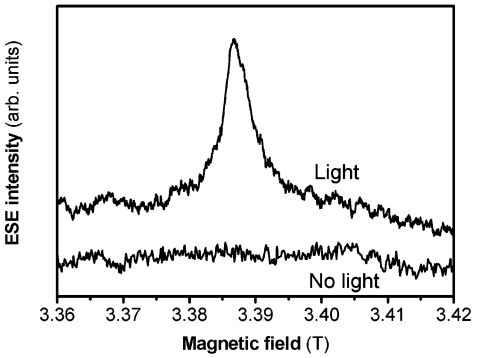

Figure 10. W-band (95 GHz) ESE-detected ESR spectra of rhodamine 6G in poly(vinyl alcohol) with (upper trace) and without (lower trace) continuous irradiation of light. The position of the resonance in the upper spectrum corresponds to the expected field for a radical.

PVA. The air we use has a relative humidity of 15%, i.e., well below 30%, the threshold above which Hou and Higgins observed significant effects on blinking.

The dark state might arise from photoinduced intramolecular rearrangement, such as the formation of a twisted intramolecular charge transfer (TICT) state. However, R6G is a reputedly stable laser dye, which to our knowledge has never been reported to undergo intramolecular photochemistry in alcoholic solution under our excitation conditions.[3,4] Furthermore, intramolecular rearrangement is not expected to occur in PVA under our experimental conditions because of its high rigidity at low relative humidity (cf. previous paragraph).[31] Remarkably, the recovery process has no activation barrier, because the lifetime of D is hardly sensitive to temperature. This once more excludes intramolecular rearrangement and all processes involving molecular diffusion of R6G or other species and most intermolecular chemical reactions involving significant rearrangements of atoms. Proton transfer is known to occur at low temperatures via tunneling, but it is usually drastically accelerated by thermal activation at room temperature. These arguments leave intermolecular electron tunneling as the most likely process for the recovery of the dark state. We are naturally led to assume that dark state D is a radical formed by intermolecular electron transfer. The family of the rhodamine dyes is known to be able to form both cationic and anionic radicals.[4,40,41] Because PVA has no electron-acceptor sites and the cation of R6G is not stable in an alcoholic environment,[4] we suppose that an electron is transferred from PVA to R6G in the lowest triplet state leading to the formation of the radical anion of R6G (see below). To emphasize the ionic character of R6G, we write Dye^+X^-,

$$[Dye^+]^TX^- + R{-}OH \leftrightarrow Dye^{\bullet}X^- + R{-}O^{\bullet+}H$$

To check whether the dark state D is indeed a radical, we perform an ESR experiment. Figure 10 shows the ESE-detected ESR spectrum of 10^{-4} M R6G in PVA at 1.5 K with and without continuous optical excitation with the green and yellow lines (546.1 and 577.0 nm) of a 100 W mercury arc. Upon illumination, a single ESR line arises at a magnetic field corresponding to $g = 2.00215 \pm 0.0001$, with a width of about 5 mT. This is the signal of a radical with $S = {}^1/_2$. The small deviation of the g-factor from that of a free electron (g = 2.002 32), approximately 0.1 mT, indicates a weak spin−orbit interaction.[33,42] This ESR line cannot stem from the triplet state of the molecule for two reasons. First, the short triplet lifetime would not allow its detection under continuous optical excitation. Second, zero-field splittings of triplet states are on the order of a few tens of millitesla,[43] which would yield a much broader ESR line with a different line shape. The ESE intensity is proportional to the number of electron spins and should therefore reflect the population of D. Under continuous irradiation, the ESE intensity increases with time and reaches a steady state after approximately 15 min (data not shown). This long rise time is due to the low intensity of the mercury arc, about 1 mW/cm^2, i.e., much lower than the intensity of the laser used in the optical experiments. When the light is switched off, the ESE signal decays back to zero, which corresponds to the recovery of the ground state of R6G. Under the same conditions no ESR signal is observed for a PVA film without R6G.

The dark state D is thus a radical pair, which reverts to S_0 by electron tunneling. To understand the distribution of the lifetimes of D, the nature of the tunneling process has to be considered. The tunneling rate mainly depends on the overlap between the wave functions of the excess electron on R6G and the hole on the PVA and therefore depends exponentially on their distance. A distribution of distances between the dye and the electron-donor site in the polymer matrix is thus expected to lead to a very broad distribution of lifetimes for D. The role of oxygen can also be understood, as oxygen may assist the recovery as an electron carrier,[3,4] which would explain the observed decrease of the lifetime of D in air.

Photoblinking processes reported earlier in the literature may also be explained by our model. Hernando et al.[44] report long off-time photoblinking (100 ms or more) of a similar rhodamine dye (TRITC, tetramethyl-rhodamine-5-isothiocyanate) incorporated in PVA, which seems to be the same process we have found in R6G. In other polymers, R6G also shows long off-time blinking, for instance in poly(methyl methacrylate),[30] a polar but hydrophobic polymer.

The formation of the radical anion of R6G from the lowest triplet state has also been observed in ethanol at room temperature,[3,4] but with a smaller rate of formation q (approximately 10^3 s^{-1}) and a higher stability of the radical, which was only affected by oxygen. The initial electron transfer to the triplet state of R6G should be equally fast in both matrixes, so that the differences probably originate from the various possible electron−hole recombination processes. The less efficient radical formation in ethanol may arise from a higher probability of immediate recombination in a fluid compared to solid PVA. The higher stability may result from the escape of the hole from

the Coulomb field of the R6G radical. The latter process appears to be negligible in PVA, even at room temperature.

Our four-level model naturally explains why the on-times in photoblinking are related to intersystem crossing, although the off-times are much longer (up to seconds) than the lifetime of the triplet state. Several authors[12,27,29] have attributed such long off-times to the triplet state. Our study rather suggests that, in many cases, the triplet state is merely the intermediate leading to a long-lived charge-separated dark state. If the temperature dependence of the off-times is weak, charge separation and recovery by tunneling are likely.

Conclusion

We have studied the photoblinking of R6G in PVA on large ensembles of molecules with continuous-wave excitation. We have measured the decay and recovery kinetics as well as the steady state of the emissivity. We have simulated our results with a kinetic model where the triplet of R6G is the intermediate between the first excited singlet state and another dark state. Because of the very weak temperature dependence of the lifetime of this dark state, we were led to assign its decay to electron tunneling. Consequently, the dark state must be a radical, which was confirmed by a light-induced ESR line at the resonant field of a free-electron. We also found a broad distribution of dark-state lifetimes, which is compatible with electron tunneling in a disordered solid matrix. Charge transfer from an excited state may be a mechanism of photoblinking that could occur in many dye−matrix couples besides R6G in PVA, in particular when off-times are longer than expected for a triplet state.

Our ensemble observations of a broad distribution of lifetimes associated with a dark state do not allow us to distinguish between two cases on the single-molecule level. First, different populations of "bright" and "dark" molecules may arise, of which the ones displaying long off-times are not expected to be observed under single-molecule conditions. Second, "bright" and "dark" periods may occur in the fluorescence time trace of each individual molecule. This case resembles the photoblinking dynamics of individual semiconductor nanocrystals.[14,15] In this sense, it is interesting to compare for R6G in PVA the results of single-molecule experiments with the present ensemble results. This is the subject of current work in our group.

Acknowledgment. We thank Jennifer Mathies and Elsbeth van der Togt for their contributions to the experiments. We acknowledge helpful discussions with Prof. W. J. Buma and Dr. E. J. J. Groenen. This work is part of the research program of the "Stichting voor Fundamenteel Onderzoek der Materie" (FOM) and is financially supported by the "Nederlandse Organisatie voor Wetenschappelijk Onderzoek" (NWO). F.K. acknowledges a Marie Curie Fellowship from the European Commission (Contract no. HPMF-CT-2001-01233).

References and Notes

(1) Moerner, W. E. *Science* **1997**, *277*, 1059.
(2) Basché, T.; Kummer, S.; Bräuchle, C. *Nature* **1995**, *373*, 132.
(3) Dempster, D. N.; Morrow, T.; Quinn, M. F. *J. Photochem.* **1973/74**, *3*, 343.
(4) Korobov, V. E.; Chibisov, A. K. *J. Photochem.* **1978**, *9*, 411.
(5) De Vries, H.; Wiersma, D. A. *J. Chem. Phys.* **1978**, *70*, 5807.
(6) Menzel, R.; Thiel, E. *Chem. Phys. Lett.* **1998**, *291*, 237.
(7) Ha, T.; Enderle, Th.; Chemla, D. S.; Selvin, P. R.; Weiss, S. *Chem. Phys. Lett.* **1997**, *271*, 1.
(8) Weston, K. D.; Carson, P. J.; Metiu, H.; Buratto, S. K. *J. Chem. Phys.* **1998**, *109*, 7474.
(9) Yip, W. T.; Hu, D.; Yu, J.; Vanden Bout, D. A.; Barbara, P. F. *J. Phys. Chem. A* **1998**, *102*, 7564.
(10) English, D. S.; Furube, A.; Barbara, P. F. *Chem. Phys. Lett.* **2000**, *324*, 15.
(11) Lu, H. P.; Xie, X. S. *Nature* **1997**, *385*, 143.
(12) Weston, K. D.; Carson, P. J.; De Aro, J. A.; Buratto, S. K. *Chem. Phys. Lett.* **1999**, *308*, 58.
(13) Deschenes, L. A.; Vanden Bout, D. A. *Science* **2001**, *292*, 255.
(14) Messin, G.; Hermier, J.-P.; Giacobino, E.; Desbiolles, P.; Dahan, M. *Opt. Lett.* **2001**, *26*, 1891.
(15) Verberk, R.; van Oijen, A. M.; Orrit, M. *Phys. Rev. B* **2002**, *66*, 233202.
(16) Orrit, M.; Bernard, J. *Phys. Rev. Lett.* **1990**, *65*, 2716.
(17) Bernard, J.; Fleury, L.; Talon, H.; Orrit, M. *J. Chem. Phys.* **1993**, *98*, 850.
(18) Basché, T.; Kummer, S.; Bräuchle, C. *Chem. Phys. Lett.* **1994**, *225*, 116.
(19) Nie, S.; Chiu, D. T.; Zare, R. N. *Science* **1994**, *266*, 1018.
(20) Veerman, J. A.; García-Parajó, M. F.; Kuipers, L.; Van Hulst, N. F. *Phys. Rev. Lett.* **1999**, *83*, 2155.
(21) Hübner, C. G.; Renn, A.; Renge, I.; Wild, U. P. *J. Chem. Phys.* **2001**, *115*, 9619.
(22) Renge, I.; Hübner, C. G.; Renn, A.; Langhals, H.; Wild, U. P. *J. Lumin.* **2002**, *98*, 91.
(23) Ambrose, W. P.; Goodwin, P. M.; Martin, J. C.; Keller, R. A. *Phys. Rev. Lett.* **1994**, *72*, 160.
(24) Ha, T.; Enderle, Th.; Chemla, D. S.; Selvin, P. R.; Weiss, S. *Phys. Rev. Lett.* **1996**, *77*, 3979.
(25) Lu, H. P.; Xie, X. S. *J. Phys. Chem. A* **1997**, *101*, 2753.
(26) Sauer, M.; Drexhage, K. H.; Lieberwirth, K. H.; Müller, R.; Nord, S.; Zander, C. *Chem. Phys. Lett.* **1998**, *284*, 153.
(27) Hofkens, J.; Maus, M.; Gensch, T.; Vosch, T.; Cotlet, M.; Köhn, F.; Herrmann, A.; Müllen, K.; De Schryver, F. C. *J. Am. Chem. Soc.* **2000**, *122*, 9278.
(28) Hou, Y. W.; Bardo, A. M.; Martinez, C.; Higgins, D. A. *J. Phys. Chem. B* **2000**, *104*, 212.
(29) Köhn, F.; Hofkens, J.; Gronheid, R.; Van der Auweraer, M.; De Schryver, F. C. *J. Phys. Chem. A* **2002**, *106*, 4808.
(30) Vargas, F.; Hollricher, O.; Marti, O.; De Schaetzen, G.; Tarrach, G. *J. Chem. Phys.* **2002,** *117*, 866.
(31) Hou, Y. W.; Higgins, D. A. *J. Phys. Chem. B* **2002**, *106*, 10306.
(32) Disselhorst, J. A. J. M.; Van der Meer, H.; Poluektov, O. G.; Schmidt, J. *J. Magn. Reson. Ser. A* **1995**, *115*, 183.
(33) Atherton, N. M. *Principles of Electron Spin Resonance*; Ellis Horwood (PTR Prentice Hall): Chichester, U.K., 1993.
(34) Gochanour, C. R.; Fayer, M. D. *J. Phys. Chem.* **1981**, *85*, 1989.
(35) Chandrasekhar, S. *Rev. Mod. Phys.* **1943**, *15*, 1.
(36) Talhavini, M.; Atvars, T. D. Z. *J. Photochem. Photobiol. A-Chem.* **1998**, *114*, 65.
(37) Talon, H.; Orrit, M.; Bernard, *J. Chem. Phys.* **1990**, *140*, 177.
(38) Gorchelev, A. A.; Snegirev, E. P.; Ulitsky, N. I.; Kharlamov, B. M. *Chem. Phys.* **2002**, *285*, 289.
(39) Stracke, F.; Heupel, M.; Thiel, E. *J. Photochem. Photobiol. A-Chem.* **1999**, *126*, 51.
(40) Ferguson, M. W.; Beaumont, P. C.; Jones, S. E.; Navaratnam, S.; Parsons, B. J. *Phys. Chem. Chem. Phys.* **1999**, *1*, 261.
(41) Navaratnam, S.; Parsons, B. J. *J. Photochem. Photobiol. A-Chem.* **2002**, *153*, 153.
(42) Krinichnyi, V. I. *Synth. Met.* **2000**, *108*, 173.
(43) McGlynn, S. P.; Azumi, T.; Kinoshita, M. *Molecular Spectroscopy of the Triplet State*; Prentice Hall, Inc.: Englewood Cliffs, NJ, 1969.
(44) Hernando, J.; Van der Schaaf, M.; Van Dijk, E. M. H. P.; Sauer, M.; García-Parajó, M. F.; Van Hulst, N. F. *J. Phys. Chem. A* **2003**, *107*, 43.